

Thermal stress involved in TRPV2 promotes tumorigenesis through the pathway of PI3K/Akt/mTOR in esophageal squamous cell carcinoma

Rongqi Huang

GIBH: Guangzhou Institutes of Biomedicine and Health <https://orcid.org/0000-0003-0456-0788>

Shuai Li

GIBH: Guangzhou Institutes of Biomedicine and Health

Chao Tian

GIBH: Guangzhou Institutes of Biomedicine and Health

Peng Zhou

Second Xiangya Hospital

Huifang Zhao

China University of Science and Technology

Wei Xie

Hunan Cancer Hospital

Jie Xiao

Central South University

Zuoxian Lin

GIBH: Guangzhou Institutes of Biomedicine and Health

Lang He

Xiangya Hospital Central South University

Xiaobo Han

GIBH: Guangzhou Institutes of Biomedicine and Health

Na Cheng

GIBH: Guangzhou Institutes of Biomedicine and Health

Feng Tang

GIBH: Guangzhou Institutes of Biomedicine and Health

Yuchen Yang

GIBH: Guangzhou Institutes of Biomedicine and Health

Hualin Huang

GIBH: Guangzhou Institutes of Biomedicine and Health

Zhiyuan Li (✉ li_zhiyuan@gibh.ac.cn)


GIBH: Guangzhou Institutes of Biomedicine and Health

Research

Keywords: ESCC, Heat stimuli, TRPV2, Tumorigenesis, PI3K

Posted Date: September 24th, 2020

DOI: <https://doi.org/10.21203/rs.3.rs-78707/v1>

License:  This work is licensed under a Creative Commons Attribution 4.0 International License.

[Read Full License](#)

Abstract

Background

Esophageal squamous cell carcinoma (ESCC) is a leading cause of cancer death worldwide. Although the exposure of esophageal mucosa to heat stimuli has long been recognized as an important risk for the initiation and development of ESCC, its underlying mechanisms remain uncharacterized.

Methods

Western blotting and immunofluorescence were used to detect the expression and localization of transient receptor potential vanilloid receptor 2 (TRPV2) in the ESCC cells. The cancerous behaviors of the ESCC cells were evaluated by a single-cell culturing assay, a wound healing assay, a 3D culturing assay and a tube formation assay respectively. In vivo tumorigenicity and metastasis of the ESCC cells were examined via xenograft nude mouse models. Western blotting and IHC were performed to determine the expression profiles of TRPV2 in the ESCC patient tissues. TRPV2 knocked-out ESCC cell line was established using CRISPR-Cas9 gene editing technique.

Results

Here, we found that the expression of TRPV2, one of the thermally sensitive TRP family members, was upregulated in both ESCC cells and clinical samples. We further showed that activation of TRPV2 by recurrent acute thermal stress (54°C, a temperature unexpectedly much lower than those in many dietary modalities) or O1821 (20 μM), a TRPV2 agonist, promoted cancerous behaviors in ESCC cells. The proangiogenic capacity of the heat-challenged ESCC cells was also found to be enhanced profoundly in the tube formation assay; both tumor formation and metastasis that originated from the cells were substantially promoted in nude mouse models upon the activation of TRPV2. These effects were inhibited significantly by tranilast (120 μM), a TRPV2 inhibitor, and abolished by TRPV2 knock-out using CRISPR-Cas9 gene editing. Conversely, overexpression of TRPV2 by transfection of TRPV2 DNA into NE2 cells, could switch the cells to tumorigenesis upon activation of TRPV2. Mechanistically, the driving role of TRPV2 in the progression of ESCC is mainly regulated by the PI3K/Akt/mTOR signaling pathway. Application of a pan-PI3K/mTOR inhibitor and/or a PTEN activator resulted in markedly reduced ESCC cell proliferation.

Conclusions

Our study first proved that TRPV2 plays an important role in the tumorigenesis of ESCC upon thermal stress. We revealed that TRPV2-PI3K/Akt/mTOR is a novel and promising target for the prevention and treatment of ESCC.

Background

Malignant disease is a leading cause of human mortality. Esophageal cancer is the 8th most frequent cancer and the 6th most common cause of cancer death worldwide, accounting for over 5.4% of all cancer-related deaths [1, 2]. The incidence is 4.5 per 100,000 individuals in the USA, while some of the highest incidences are found in Southeastern Africa and the so-called Asian esophageal cancer belt (Turkey, Iran, Kazakhstan, and Northern and Central China) [3, 4], with approximately 100 per 100,000 individuals affected, more than 480,000 new cases diagnosed and 400,000 deaths yearly. Esophageal squamous cell cancer (ESCC) comprises the majority of esophageal malignancies (~ 90%), followed by adenocarcinomas [5]. In China, both the incidence and mortality of ESCC rank 4th among all cancers. ESCC remains one of the most lethal cancers among all malignancies, with a 5-year survival rate of < 20% once diagnosed [6]. Reasons may be the lack of a sensitive method for early detection; thus, detectable regional and distant metastasis have occurred in most ESCC patients at the time of diagnosis [7, 8], and the limited clinical staging criteria lacks significant molecular biomarkers to effectively stratify patients for treatment options [9].

The pathogenesis of the disease has been suggested to be multifactorial, while the most important risk factors for ESCC are thought to be environmental, including tobacco smoking, alcohol drinking, dietary carcinogens (nitrosamines), insufficiency of micronutrients, exposure to polycyclic aromatic hydrocarbons (PAHs), and hot beverage consumption [10–13]. Consumption of beverages and food at high temperatures, which expose the esophageal mucosa to heat stimuli, has been documented to increase the risk of ESCC [14], and heat stimuli have been ranked as cause classification II for ESCC by the International Association of Cancer Registries (IACR) [15]. Pooled analysis adds evidence for a carcinogenic effect of chronic thermal injury in the esophagus induced by the consumption of very hot drinks, including mate [16]. However, the underlying mechanism is poorly understood.

In this study, we found that transient receptor potential vanilloid receptor 2 (TRPV2), a member of the thermosensitive TRPV channels, was upregulated in ESCC cells compared to non-tumor esophageal squamous cells (NE2) and in clinical ESCC samples in comparison with adjacent non-tumor tissues. Furthermore, recurrent acute challenging of the cells with heat stimuli (54 °C, it is much lower than the dietary temperatures among many populations, but it could activate the TRPV2 channel in the cells) [17–19] significantly enhanced ESCC cancerous behaviors (proliferation, migration, invasion, and angiogenesis) in vitro and markedly promoted tumorigenesis (tumor formation and metastasis) in vivo. The aggressiveness of ESCC cells was also augmented substantially upon the pharmaceutical activation of TRPV2. However, the tumorigenesis of ESCC was attenuated considerably by either inhibition of TRPV2 with tranilast (120 µM) (an antagonist of TRPV2) or TRPV2 knockout using CRISPR-Cas9. In contrast, overexpression of TRPV2 by transfection of a plasmid containing TRPV2 DNA into the non-tumor esophageal squamous cells (NE2), could switch the cells to tumorigenesis upon activation of TRPV2. Mechanistically, the role of TRPV2 in the progression of ESCC was found to be regulated by HSP and PI3K signaling pathways. Application of VS5584 (a pan-PI3K/mTOR kinase inhibitor) or oroxin B (a PTEN protein activator and PI3K/mTOR inhibitor) resulted in remarkably reduced proliferation of ESCC cells. Together, our findings reveal a novel and important role of TRPV2 playing in the progression of

ESCC upon thermal stress and identify the TRPV2-PI3K/Akt/mTOR pathway as a potential target for the prevention and treatment of ESCC.

Materials And Methods

Plasmids and chemicals

pCMV6-TRPV2 and pCMV6-GFP were obtained from OriGene and maintained by our lab. O1821 and VS-5584 were purchased from Cayman Chemical and MedChemExpress, respectively. Tranilast and oroxin B were both obtained from TargetMol. The chemicals were dissolved in DMSO (the maximal final concentration of DMSO was never exceeded 0.1% throughout the study) and diluted in PBS or extracellular solutions (pH 7.4) to obtain the desired concentrations. Agonist and antagonists were used at the concentrations based on our pre-experiments on ESCC cells. Matching volumes of DMSO were used as controls.

Cell culture

The human esophageal squamous cell carcinoma (ESCC) cell lines Eca-109 and TE-1 were obtained from the Cell Bank of the Chinese Academy of Sciences (Shanghai, China). Eca-109-gf (GFP and luciferase dually labeled Eca-109) cell line, Eca-109-VR2^{-/-} (TRPV2 knocked-out Eca-109) cell line and Eca-109-VR2^{-/-}-gf (TRPV2 knocked-out and GFP- luciferase dually labeled Eca-109) cell line were established and maintained by our group. The ESCC cells were cultured in RPMI medium 1640 (Thermo Scientific, MA, USA) supplemented with 1 mM L-glutamine, and 10% (vol/vol) FBS. The immortalized normal esophageal squamous cell line NE2 (kindly provided by Prof. GSW Tsao, Hong Kong University), was cultured in a 1:1 ratio of Defined Keratinocyte-SFM (DKSFM) supplemented with growth factors (Thermo Scientific, MA, USA) and Epi-life medium supplemented with Epi-life Defined Growth Supplement (EDGS) growth factors (Thermo Scientific, MA, USA). HUVECs were obtained from American Type Culture Collection and were maintained in DMEM (Thermo Scientific, MA, USA) supplemented with 10% (vol/vol) FBS. Cell lines were authenticated using short tandem repeat profiling by the direct suppliers or by our institute (HUVECs). Routine *Mycoplasma* testing was performed by MycoAlert Mycoplasma Detection Kit (#LT07-318, Lonza) every 3 to 6 months. Cells were cultured in a humidified incubator with 5% CO₂ at 37 °C. Unless otherwise indicated, the medium was replaced every 3 days, and the cells were subcultured when they reached 85% confluence.

Soft-agar assay

Anchorage-independent growth was determined in 0.33% agarose (BioWest, Nuaille, France) with a 0.5% agarose underlay in 60 mm dishes.

Intracellular calcium imaging

Cells were cultured in 3 cm-diameter glass-bottom dishes for 24 h, thereafter medium was discarded and dishes were washed using 4°C Hank's balanced salt solution (HBSS), then cells were pre-incubated with 5 μ M Fura-2-AM (Dojindo Laboratories) in 1 ml HBSS in the dishes for 45 min at 37°C in dark.

Subsequently, the pre-incubated solution was pipetted away and cells were washed three times with HBSS to eliminate the extracellular Fura-2AM, then 1ml of HBSS was added and cells were incubated at 37°C in dark for 20 min for the full de-esterification of intracellular Fura-2AM, then calcium imaging was performed as we described previously [20].

Protein extraction and western blotting

Protein extraction from cell lines and patient tissues and western blotting was performed as previously described [20, 21]. Primary antibodies including rabbit anti-human TRPV2 (#sc-30155, Santa Cruz), rabbit anti-human β -Actin (#5125, CST), rabbit anti-human HIF1 (#A11945, Abclonal), rabbit anti-human TNF α (#A0277, Abclonal), rabbit anti-human NF κ B (#A11163, Abclonal), rabbit anti-human HSP27 (#A0240, Abclonal), rabbit anti-human HSP40 (#A5504, Abclonal), rabbit anti-human HSP60 (#A0969, Abclonal), rabbit anti-human HSP70 (#A0284, Abclonal), rabbit anti-human HSP90 (#A1087, Abclonal), rabbit anti-human Calmodulin (#abs133163, Absin), rabbit anti-human PTEN (#abs134055, Absin), rabbit anti-human AKT1 (#sc-5298, Santa Cruz), rabbit anti-human PI3K (#A0265, Abclonal), rabbit anti-human PDK1 (#abs131621, Absin) and rabbit anti-human mTORC1 (#sc-517464, Santa Cruz) were applied according to manufacturer's instructions. Horseradish peroxidase-linked secondary antibodies (goat anti-rabbit IgG, Beyontime, Nanjing, China) were used.

Immunofluorescence analysis and microscopy

The cells were processed before being subjected to immunofluorescence analysis as described previously [20]. Rabbit anti-human TRPV2 primary antibody (#sc-30155, Santa Cruz) and Alexa Fluor 594 goat anti-rabbit secondary antibody (#ab-150080, Abcam) were used according to the manufacturers' instructions.

Plasmid DNA transfection

An NE2 cell suspension of 2.5×10^6 cells/ml in electroporation buffer was mixed with a 3 μ g/ μ l pCMV6-TRPV2 and pCMV6-GFP solution at a 4:1 ratio to a final concentration of 0.6 μ g/ μ l for each pDNA. Then the mixture was transferred into a cuvette. Transfection was achieved by electroporation with the NeonTM transfection system (Life technology) at 1350 V, 30 ms, 1 pulse. Subsequently, the cells were immediately transferred into the wells of a 6-well culture plate containing 2 ml of medium/well to ensure proper cell recovery. The plate was incubated at 37°C in 5% CO₂ for further experiments.

gRNAs and CRISPR/Cas9 vectors

The protocols for sgRNA design, vector construction and in vitro transcription were conducted according to previously published protocols [23]. First, the sgRNAs targeting the human TRPV2 gene (NC_000017.11) were designed using the online CRISPR Design Tool (<http://crispr.mit.edu/>). Then, the

complementary oligo sgRNAs were cloned into the BbsI sites of a Puc57-T7-sgRNA cloning vector (Addgene ID51306). The amplified PCR products of the Puc57-T7-sgRNA vector were transcribed in vitro using the MAXIscript T7 Kit (Ambion) and purified with the miRNeasy Mini Kit (Qiagen) according to the manufacturers' instructions.

Off-target analysis

The POT sites for each sgRNA were predicted to analyze site specific edits by the BE3 system according to an online design tool (<http://www.rgenome.net/cas-offfinder/>) [24]. All POTs were amplified by PCR and then subjected to Sanger sequencing to confirm the off-target effects, respectively. The primers for amplifying the off-target sites are listed in Additional file 8: Table S1.

Drug administration and thermal stimulation protocol

Cells were pretreated with the indicated dose of TRPV2 activator and/or inhibitors (dissolved and remained in culture medium until next medium renewal, medium was replaced twice per day) or exposed to heat (54°C) stimulation (water bath, thrice per day, 30 seconds per time) or heat (54°C) stimulation and/or tranilast (120 µM), VS5584 (95 nM) or oroxin B (156 nM) respectively for up to 14 days. Heat stimulation was performed as described previously [20].

Cell proliferation assay

Cell proliferation was evaluated via a single-cell culture assay. Cells following treatment as described in *Drug administration and thermal stimulation protocol* were trypsinized, then suspended and diluted to a concentration of 1 cell per 10 µl. Subsequently, 10 µl of each cell suspension was seeded per well in a 48-well culture plate. The seeded cells were observed under an inverted microscope (Nikon) and wells with more than 1 cells were excluded from the assay. The cell numbers were counted manually under the inverted microscope or by imaging all the cell clones and further processed via ImageJ software.

Cell wound healing assay

Four parallel lines were drawn on the back of the 6-well plates with a marker pen before cell seeding. Cells following the treatment as described in *Drug administration and thermal stimulation protocol* were applied and wound healing assay was conducted as described previously [20].

Three-dimensional invasion assay

AIM chips (AIM Biotech, Singapore) were assembled according to the manufacturer's instructions. Matrigel (#354248, Corning) was used to fill the gel tunnel from one side all the way to the other side. The gel-filled chips (on AIM holders) were placed into a 37 °C incubator and incubated for 30 min to allow polymerization of Matrigel. Cells following the treatment as described in *Drug administration and thermal stimulation protocol* were trypsinized and diluted to a density of 1×10^6 . A micropipette was used to withdraw 10 µl of cell suspension. The tip was directed near the inlet of the medium channel and the cell

suspension was injected. After 2 min, the same procedure was repeated for the opposite connecting inlet. In total, 20 μ l of cell suspension was seeded per medium channel. To exchange medium in a medium channel, 70 μ l of medium was added into one port and then 50 μ l was added to the opposite connecting port. Cells were filled and allowed to invade into the gel tunnel and were visually inspected under an inverted microscope (Nikon); invaded cells were manually counted in 10 fields and compared. Furthest distances of the invaded cells (away from the starting point) were measured and compared.

Tube formation assay

Eca-109 and Eca-109-TRPV2^{-/-} cells followed the indicated treatment as described in *Drug administration and thermal stimulation protocol* were cultured in 6-well plates with 2 ml fresh serum-free medium for 24 hours, then 24 hours' conditioned medium was collected for tube formation assay. A 48-well plate was pre-coated with 125 μ l Matrigel (#354248, Corning) and allowed to solidify at 37°C for 1 h. Then HUVECs (1×10^5) resuspended with conditioned medium were layered onto the Matrigel and monitored over time for the formation of tube-like structures. Endothelial cell formation was observed, and photos were captured 48 h later under an inverted microscope (Nikon). Relative quantities of the tubules were quantified by ImageJ software.

In vivo tumorigenicity and metastasis assay

Male BALB/c nude mice (3–4 weeks of age, 18–20 g) were purchased from Vital River Laboratories. All of the animal studies were conducted under protocols approved by the guidelines of the Ethics Committee of Animal Experiments at GIBH. The BALB/c nude mice were randomly divided into 6 groups ($n = 4–7$ mice/group). Five million Eca-09 cells following the treatment as described in *Drug administration and thermal stimulation protocol* were mixed at a ratio of 1:1 (v/v) with Matrigel (#354248, Corning) and injected subcutaneously into the left flank of 4- to 5-week-old male BALB/c nude mice. Tumor volumes were determined every 3 days, and were calculated using the equation $0.52 \times a \times b^2$, where a and b are the largest and smallest lengths of the tumor, respectively. GFP and luciferase (GL)-expressing tumor cells (Eca-109-gl, 1×10^5) were i.v. through the tail vein into BALB/c nude mice to establish metastatic models. To generate bioluminescence signals, D-luciferin (3 mg/100 μ l per mouse, Yeasen Biotech, Shanghai, China) was injected i.p. 5 min before the image acquisition. Image data were acquired by 15 s exposure using the IVIS Spectrum at an interval of 2 wks and analyzed using the Living Image software (PerkinElmer). On day 45 or 49, animals were euthanized, and tumors were excised, weighed, photographed and lungs were paraffin embedded for further experiments.

IHC, and hematoxylin and eosin (HE) staining of mouse tissues

Serial 4.0- μ m lung sections were cut and subjected to IHC staining using an anti-Ki-67 (#abs131599, Absin, Shanghai, China) and anti-CD31 antibody ((#abs131735, Absin, Shanghai, China) or H&E stained with Mayer's hematoxylin solution. IHC and H&E staining were performed according to standard protocols. The images were captured using the Computerized Image Analysis System (Carl Zeiss). The

microvessel density (MVD) was quantified by counting the proportion of CD31-positive cells. The proliferation index was quantized by counting the proportion of Ki-67-positive cells.

Fresh clinical tissue specimen collection and processing

Fresh human esophageal squamous tumors and adjacent non-tumor tissue specimens were obtained from 35 patients undergoing esophageal resection for ESCC (4 patients with poor sample quality were later excluded from the trial). For the use of these clinical materials for research purposes, prior patient consent and approval from the Institutional Research Ethics Committee were obtained. Specimens were collected between 2017 and 2018 at the Cancer Hospital of Hunan Province in Changsha, China. Samples were transferred to our lab via cold-chain transportation and prepared for further experiments. The clinical information of the patients is summarized in Additional file 9: Table S2.

Human esophageal cancer tissue specimens and IHC

We obtained paraffin-embedded tissue samples in accordance with the ethical standards of the Institutional Committees on Human Experimentation from 193 consecutive patients with esophageal squamous cell carcinoma who had undergone surgery without preoperative chemotherapy or radiotherapy between 2012 and 2013 at the Second Affiliated Hospital of Xiangya Medical School of Central South University, Changsha, China. Corresponding specimens from each patient's distant (5 cm from the tumor lesions) normal tissue were also collected in each case. Serial 3.0 ~ 4.0- μ m sections were cut and subjected to IHC staining using an anti-TRPV2 antibody (#sc-30155, Santa Cruz). The clinical information of the patients is summarized in Additional file 9: Table S2.

Statistical Analysis

Results are presented as mean \pm SD. Data were analyzed by one-way ANOVA or two-way ANOVA followed by Bonferroni's post hoc test unless otherwise stated. All data and statistical analysis were performed by Origin 9.1 or GraphPad Prism 8 software. $P < 0.05$ was considered statistically significant. Asterisks indicate statistical difference as follows: ns, not significant; * $P < 0.05$; ** $P < 0.01$; *** $P < 0.001$.

Results

TRPV2 is upregulated in ESCC cells, and overactivation of TRPV2 promotes cell proliferation

Transient receptor potential vanilloid receptor 2 (TRPV2) is functionally thermosensitive and can be activated by heat at high temperature ($> 52^{\circ}\text{C}$) [25]. To explore the expression of TRPV2 in ESCC cells (Eca-109 and TE-1) and non-tumor esophageal squamous cells (NE2) (the anchorage-independent growth of the cell lines was tested by a soft agar colony formation assay, Additional file 1: Figure S1a), we conducted western blotting. TRPV2 protein (86 kDa) was detectable among all three cell lines, and the expression of TRPV2 was found to be upregulated in ESCC cells compared with NE2 cells (Fig. 1a-b). To further examine the expression and localization of TRPV2 among these cell lines, immunocytofluorescence was carried out. TRPV2 was found to be expressed and localized

predominantly in the plasma membrane of ESCC cells and NE2 cells (Fig. 1c and Additional file 1: Figure S1b).

Cellular proliferation viability was evaluated via a single-cell culturing assay, based on previous studies that tumors could originate from a single cell and further grow uncontrollably, eventually leading to a malignant state [26, 27] and our observation that tumor cells are more tolerant of 'unfavorable' conditions than non-tumor cells, therefore they could survive an extremely scarce nutritious environment.

Cellular proliferation of Eca-109 was promoted significantly upon exposure to recurrent brief heat stimuli (54°C) or frequent application of O1821 (20 µM), which could activate TRPV2, as confirmed by a calcium imaging assay (Additional file 2: Figure S2a-l). In this study, the term 'overactivation' was used to describe the abovementioned patterns of heat treatment (54°C) or the application of O1821 (20 µM), which could cause frequent activations of TRPV2. The pro-proliferative effects on Eca-109 cells were abrogated by either simultaneous application of tranilast (120 µM), a TRPV2 antagonist, or by TRPV2 knockout using CRISPR-Cas9 (Fig. 1d-f). Similar effects could be observed in another ESCC cell line, TE-1 (Additional file 3: Figure S3a-b). It is worth noting that cellular proliferation of Eca-109 was decreased substantially by the knock-out of TRPV2. The proliferation of wild-type NE2 (NE2-WT, which was with low expression level of TRPV2, Fig. 1a-b) cells was affected by neither exposure to recurrent brief heat stimuli (54°C) nor

application of O1821 (20 µM) (Fig. 1g and Additional file 3: Figure S3c). Conversely, when the proliferation assay was conducted on NE2 cells with ectopically expressed TRPV2 (NE2-VR2), the cellular proliferation of NE2 cells was enhanced markedly upon exposure to recurrent brief heat stimuli (54°C) or O1821 (20 µM), and these effects were attenuated by tranilast (120 µM) (Fig. 1h and Additional file 3: Figure S3d). Together, these data indicated that overactivation of TRPV2 could promote the proliferation of esophageal squamous cells and upregulation of TRPV2 might play a role in the pathology of ESCC.

Overactivation of TRPV2 enhances the migration and invasion of ESCC cells in vitro

To assess the impact of TRPV2 activation on ESCC cell migration, a wound healing assay was applied. Cellular migration of ESCC cells (Eca-109 and TE-1) was considerably accelerated upon the activation of TRPV2 by recurrent brief heat (54°C) stimuli or administration of O1821 (20 µM), and these effects were abolished by either the TRPV2 antagonist, tranilast (120 µM), or by TRPV2 knockout using CRISPR-Cas9 (Fig. 2a-b and Additional file 4: Figure S4a-b). These data suggested that overactivation of TRPV2 could promote the migratory ability of ESCC cells. On the other hand, the migratory ability of wild-type NE2 cells (NE2-WT, which had a low expression level of TRPV2, Fig. 1a-b) remained unaffected upon the overactivation of TRPV2 by heat (54°C) stimuli or O1821 (20 µM) treatment (Fig. 2c and Additional file 4: Figure S4c). Conversely, cellular migration was enhanced profoundly upon the overactivation of TRPV2 by both cues in the NE2 cells with ectopically overexpressed TRPV2 (NE2-VR2) (Fig. 2d and Additional file 4: Figure S4d), hence further verifying the promigratory role of TRPV2 in the cells.

To evaluate the cellular invasive process, we used a new platform adopting AIM 3D chips [28]. The trajectory of invasive cells can be monitored over time during the experiments, and the invasive process

(including invasive cell numbers and furthest invaded distance by the most front cell) can be easily visualized and measured using these chips in the assay, compared with the traditional way of using Boyden chambers [29-31]. The number of invasive ESCC cells (Eca-109 and TE-1) and the furthest invaded distance of these cells were enhanced markedly by recurrent brief heat (54°C) stimuli or exposure to O1821 (20 µM), and these effects were attenuated significantly by tranilast (120 µM) or by TRPV2 knockout using CRISPR-Cas9 (Fig. 2e-f and Additional file 5: Figure S5a-c). It is noteworthy that both cellular migration and invasion of Eca-109 cells was significantly inhibited by the knockout of TRPV2 ((Fig. 2a-b, e-f and Additional file 5: Figure S5a, c). Taken together, these findings suggested that overactivation of TRPV2 could promote the migratory and invasive ability of ESCC cells.

For the non-tumor line, the invasive ability (including invasive cell numbers and furthest invaded distance) of wild-type NE2 (NE2-WT) cells were affected neither by the overactivation of TRPV2 by recurrent brief heat stimuli (54°C) nor by O1821 (20 µM) treatment, whereas the invasive ability (including invasive cell numbers and furthest invaded distance) of ectopically expressed TRPV2 NE2 (NE2-VR2) cells was elevated substantially upon the overactivation of TRPV2 by recurrent brief heat stimuli (54°C) or O1821 (20 µM) administration. Again, these effects were abolished by tranilast (120 µM) (Fig. 2g and Additional file 5: Figure S5c), which further corroborates the pro-invasive role of TRPV2.

Overactivation of TRPV2 in ESCC cells promotes tumor-related angiogenesis

The capability to promote angiogenesis within or surrounding the tumor tissue is a hallmark of many oncogenic factors [32]. To examine the impact of TRPV2 overactivation in ESCC cells on angiogenesis, a tube formation assay was applied (Fig. 3a). Human umbilical vein endothelial cells (HUVECs) were used as angiogenesis progenitor cells. The recruitment of HUVECs and the total length of newly formed microvessels were all significantly promoted by conditioned medium derived from Eca-109 cells following the overactivation of TRPV2 by recurrent brief heat stimuli (54°C) or the treatment with O1821 (20 µM), and these effects were attenuated remarkably by tranilast (120 µM). Meanwhile, the pro-angiogenic effect (on the total length of newly formed microvessels) of the conditioned medium derived from Eca-109-VR2^{-/-} (TRPV2 knocked-out Eca-109) cells following recurrent brief heat stimuli (54°C) was arrested (Fig. 3b-c). Furthermore, the number of junctions and branches of the newly formed microvessels was also significantly increased by the conditioned medium derived from Eca-109 cells following the overactivation of TRPV2 by recurrent brief heat stimuli (54°C) or by the administration of O1821 (20 µM), and these effects were markedly inhibited by tranilast (120 µM). Conditioned medium derived from Eca-109-VR2^{-/-} cells following recurrent brief heat stimuli (54°C) induced much less microvessel formation (with much fewer junctions and branches of the newly formed microvessels) versus the control in the assay (Fig. 3b, d-e). Collectively, these findings indicated that overactivation of TRPV2 could promote tumor-related angiogenesis in ESCC cells and thus might promote the tumorigenesis of ESCC.

Overactivation of TRPV2 promotes ESCC growth and invasion in xenograft models

The biological role of TRPV2 in ESCC progression in vivo was investigated using BALB/c nude mice to generate a tumor xenograft model. In the ESCC formation assay, the tumors originating from Eca-109 cells followed recurrent brief heat (54°C) challenge or O1821 (20 μM) application were significantly larger, in both size and weight, than the tumors from control cells, and these effects were attenuated markedly by tranilast (120 μM) (Fig. 4a–c). Notably, the tumors formed by TRPV2 knockout cells (Eca-109-VR2^{-/-}) followed recurrent brief heat (54°C) treatment were clearly smaller and had substantially lower tumor weights than the tumors formed by control cells (Fig. 4a–c). By contrast, wild-type NE2 cells were subcutaneously injected into the BALB/c nude mice, but no tumor formation was found even up to 30 days post inoculation. Conversely, when we used ectopically expressed TRPV2 NE2 (NE2-VR2) cells (Additional file 6: Figure S6a-b) to perform the similar experiments, on day 12 after inoculation, tumors were palpable in the groups which were subcutaneously injected with NE2-VR2 cells followed recurrent brief heat (54°C) challenge or O1821 (20 μM) application. To the end of the assay, it was observed that overactivation of TRPV2 by recurrent brief heat (54°C) challenge or O1821 (20 μM) treatment could significantly promote tumor formation, which was displayed with larger tumor sizes and greater tumor weights compared to the control group, and these effects were compromised markedly by tranilast (120 μM) (Additional file 6: Figure S6c-e). These findings further verified that overactivation of TRPV2 could significantly promote ESCC tumor formation in nude mouse models.

Moreover, an experimental tail vein metastasis model was established using BALB/c nude mice. The photon flux of Eca-109-gl cells (GFP and luciferase dual-labeled Eca-109 cells) followed recurrent acute heat (54°C) challenge or O1821 (20 μM) administration to the lungs was profoundly enhanced compared with that in the control group, and these effects were attenuated significantly by tranilast (120 μM) application or by TRPV2 knockout using CRISPR Cas9 (Fig. 4d and Additional file 6: Figure S6f), suggesting that overactivation of TRPV2 markedly promotes the ability of Eca-109-gl cells to metastasize to the lungs following cell injection through the tail vein. Lungs derived from the group followed overactivation of TRPV2 in ESCC cells by recurrent acute heat (54°C) challenge showed more metastatic tumor nodules than lungs from the control group (the rightmost panel of Fig. 4d). Consistently, the H&E staining of the lungs showed clear tumor lesions in the group followed over-activation of TRPV2 in the ESCC cells by recurrent acute heat (54°C) challenge, whereas tumor lesions were attenuated markedly by tranilast (120 μM). Meanwhile, tumor lesion was nearly absent from the TRPV2 knockout (Eca-109-gl-VR2^{-/-}) group (Fig. 4e). Immunohistochemical analysis revealed that the group followed overactivation of TRPV2 in ESCC cells by recurrent acute heat (54°C) challenge showed markedly increased percentages of Ki-67-positive cells and of CD31-positive cells (which represents the proliferative cells and the newly formed microvessels respectively) compared to those of the control group (Fig. 4e-g). When combined with tranilast (120 μM), the group followed over-activation of TRPV2 in ESCC cells by recurrent acute heat (54°C) challenge demonstrated much smaller Ki-67 proliferation indices and weaker newly formed microvessels signals (Fig. 4e-g), implying that overactivation of TRPV2 could promote tumor proliferation and tumor-related angiogenesis in vivo. Moreover, ESCC tumor formation under the skin, tumor metastasis to the lungs, the proliferation index and newly formed microvessels signal of the

mouse lungs were all reduced by the knockout of TRPV2 (Fig. 4), further supported the notion that the driving role of TRPV2 in the progress of ESCC.

To sum up, these data suggest that the overactivation of TRPV2 contributes to the augmented proliferative, angiogenic and metastatic capacity of ESCC cells and hence drives ESCC progression in vivo.

Overactivation of TRPV2 activates HSP and PI3K/Akt/mTOR signaling pathways

To explore the mechanism(s) underlying the role that overactivation of TRPV2 plays in the progression of ESCC, western blotting was carried out. Eca-109 cells were treated as described in *Drug administration and thermal stimulation protocol* (see *Methods*) prior to western blotting assay.

It is well known that HSF1 (heat shock factor 1) mediates heat shock stress within organisms; therefore, we tested whether HSF1 is involved in the heat treatment of the ESCC cells. As expected, HSF1 was upregulated by overactivation of TRPV2 by heat stimuli (54°C), and this effect was inhibited by tranilast (120 µM) or TRPV2 knockout using CRISPR-Cas9 (Fig. 5e-f), indicating that HSF1 was modulated during the overactivation of TRPV2 by heat.

Next, five members of the HSP family, including HSP27, HSP40, HSP60, HSP70, HSP90, were examined during the assay, and only HSP70 and HSP27 were found to be upregulated by overactivation of TRPV2 upon exposure to heat stimuli (54°C) or O1821 (20 µM) (Fig. 5a-c, e-f). The expression levels of both proteins were returned to near baseline when the activation was antagonized by tranilast (120 µM), suggesting that the expression of these HSP proteins was mediated by TRPV2 (Fig. 5a, c, e-f). Previous works had reported that these two HSP proteins are involved in the progression of multiple types of cancers [33-35]. HSP70 and HSP27 may also play a role in the tumorigenesis of ESCC following the overactivation of TRPV2. The expression levels of calmodulin were inversely proportional to the overactivation of TRPV2 (Fig. 5b, d), possibly because more calmodulin protein was employed to modulate the increased influx of Ca²⁺ following overactivation of TRPV2, which is consistent with the results of Ca²⁺ imaging assays (Additional file 2: Figure S2a-b, e-f).

Given that noxious heat stimulation may induce inflammatory reactions, we then measured two important inflammation-related pathways, PI3K and NFκB. The expression of PI3K was enhanced with the overactivation of TRPV2 by either heat stimuli (54°C) or O1821 (20 µM), and these effects were inhibited by the TRPV2 inhibitor tranilast (120 µM) or by TRPV2 knockout using CRISPR Cas9, whereas the expression of NFκB remained unchanged during the overactivation of TRPV2 (Fig. 5e-f), suggesting that PI3K may be involved in the overactivation of TRPV2, while NFκB is not.

To further investigate the PI3K pathway playing in the progression of ESCC driven by overactivation of TRPV2, we measured the expression of up- and downstream signaling proteins of this pathway. PDK1, which can be activated by PI3K, was found to be upregulated upon overactivation of TRPV2, and as expected, AKT1 and mTORC1, the target proteins of PDK1, were accordingly upregulated by

overactivation of TRPV2 (Fig. 5g-h). In contrast, PTEN, the negative regulatory protein of PI3K, was conversely regulated during the process of overactivation of TRPV2 (Fig. 5g-h), suggesting that the PI3K signal was activated during the overactivation of TRPV2 and may be amplified by PTEN, thus significantly promoting the aggressiveness of ESCC upon overactivation of TRPV2.

In addition, it is worth noting that TNF α was upregulated by heat stimuli, while this effect may not be regulated by TRPV2 because its expression remained unchanged when tranilast (120 μ M) was simultaneously applied or TRPV2 was knocked-out using CRISPR-Cas9 (Fig. 5e-f). The activation of TNF α results in cell death [36]. Indeed, we did observe a small portion of cell death during the heat stimulation process, while the overall cell numbers were not decreased but increased in response to overactivation of TRPV2 (Fig. 1d, f), suggesting that both pro-cell death and pro-cell proliferation signals could be simultaneously activated during the process of overactivation of TRPV2 by heat stimuli, while the latter signal exceeded the former, thus leading to the substantial increase in ESCC cell numbers upon overactivation of TRPV2.

Last, to further confirm the role of TRPV2-PI3K/Akt/mTOR playing in the progression of ESCC, VS5584 (a pan-PI3K/mTOR kinase inhibitor) and oroxin B (a PTEN protein activator and a pan-PI3K/mTOR kinase inhibitor) were applied in the Eca-109 cellular proliferation assay. As expected, both compounds could significantly attenuated Eca-109 proliferation following overactivation of TRPV2 by frequent acute heat (54°C) challenge or O1821 application (Additional file 7: Figure S7a-b). Thus, we further verified the driving role of the TRPV2-PI3K/Akt/mTOR axis in the progression of ESCC. Taken together, these data suggest that the HSP and PI3K/Akt/mTOR signaling pathways participate in the overactivation of TRPV2 and may play an important role in the tumorigenesis of ESCC upon the overactivation of TRPV2 (Additional file 7: Figure S7c).

TRPV2 is upregulated in ESCC tumor tissues

To ask the question of whether tumor tissues from patients have similar TRPV2 expression patterns to the ESCC cells used in the present study, we performed western blotting on 31 fresh samples derived from ESCC patients to detect the expression of TRPV2 protein and conducted IHC on 193 pathological slides of ESCC patients obtained from multiple hospitals (patient information is shown in Additional file 9: Table S2).

As expected, upregulation of TRPV2 was found in over 87% (27 out of 31 cases) of the fresh ESCC tissues compared with their matched adjacent non-tumor tissues (Fig 6a-c). The staining of TRPV2 in the IHC assay showed that, in comparison to the non-tumor tissue, upregulation of TRPV2 was found in 84.1% of ESCC tumor tissues compared with adjacent non-tumor tissues (Fig 6d, f). Intriguingly, the expression of TRPV2 was found to be upregulated among 77.5% of the squama of the para-tumor in the tumor slides compared with that of the non-tumor slides (Fig 6e, g). Further efforts are needed to identify whether TRPV2-positive cells in the squama of those para-tumor tissues are transformed or untransformed cells.

Discussion

In this study, we found that a member of the temperature-sensitive transient receptor potential vanilloid receptor subfamily, i.e., TRPV2, was upregulated in esophageal squamous cell carcinoma (ESCC) cell lines and clinical ESCC samples compared with non-tumor control subjects. Further, the TRPV2 protein was found to be predominantly localized to the plasma membrane of the cells and was functionally active. Since TRPV2 is a noxious heat-activated ion channel validated by previous works, and exposure of the esophageal mucosa to heat stimuli has been believed to be an important risk factor for the initiation and development of ESCC [14, 37, 38], we tested the impact of activation of TRPV2 by thermal stimuli (54 °C) and a chemical agonist (O1821, 20 μM) on the cancerous behaviors of ESCC cell lines including cellular proliferation, migration and invasion. We found that the overactivation of TRPV2 by recurrent brief thermal stimuli or O1821 application could significantly promote all these malignant behaviors, indicating that TRPV2 plays a role in the development of ESCC.

In the present study, we developed a new method, i.e., single-cell culturing method, to evaluate cellular proliferation of ESCC cells. Although many hold that cancer may be originated from a very small portion of cancer stem cells (CSC) [39–41], during our experiments, we found that even a single ESCC cell could survive the extremely unfavorable culturing conditions and continues to be proliferative (they can survive an 'old' medium which was not renewed for as long as 35 days, while non-tumor cells such as NE2 cells could not survive this condition for longer than 1 week). Therefore, it is feasible to examine cellular proliferation at single-cell level and it will be more precise than conventional methods (such as methods using MTT and CCK8) on evaluation of the proliferation viability of cancer cells. Furthermore, it is comparable with the traditional CCK8 method. It would be more precise to investigate pro-tumorigenic factors, to test new chemicals on cancer cells or to predict therapeutic regimens using this single-cell culturing method. Nevertheless, more efforts are needed to prove its practicality on the culturing of other types of cancer cells. Additionally, we applied a set of 3D culturing chips devised by MIT researchers [42] to the cellular invasion assay. Three-dimensional culturing could better mimic *in vivo* cancer microenvironment and will be better in predicting the outcome of a cellular invasion assay [43–45]. Therefore, together with others, we propose that 3D culturing is a better option to assess the invasive ability of cancer cells [46, 47].

The pro-angiogenic process of cancer cells is believed to be an important step in tumor growth and development [32, 48]. Herein, we found that overactivation of TRPV2 could markedly promote angiogenesis in the tube formation assay, thus further support that the pro-tumorigenic role of TRPV2 in the progression of ESCC may partly attribute to its pro-angiogenic potential.

When we translated the outcomes to an *in vivo* assay, we found that overactivation of TRPV2 could substantially promote both xenograft tumor formation under the skin through subcutaneous injection and tumor metastasis to the lungs via tail injection, the signals of the proliferative cells (Ki-67-positive) and newly formed microvessels (CD31-positive) were significantly upregulated, whereas pharmacological inhibition of TRPV2 and especially TRPV2 knockout using CRISPR-Cas9 showed clearly reduced tumor

formation, metastasis and related indices in vivo, which is consistent with and further verified the pro-malignant behaviors observed during the in vitro experiments. It is worth noting that, multiple malignant behaviors of the Eca-109 cells were sufficiently attenuated by the knockout of TRPV2 using CRISPR Cas9 technique, it might imply, from the loss of function's (LOF) perspective, that TRPV2 may be oncogenic *per se*.

Conversely, the wild-type non-tumor cell line NE2 did not show any of these properties; however, when TRPV2 was overexpressed by transfection of the TRPV2 plasmid into the wild-type cells (to establish NE2-VR2 cells), we found that the overactivation of TRPV2 in NE2-VR2 cells could promote markedly cellular proliferation, migration, and invasion of the cells. Tumor formation also was observed by subcutaneously injecting these cells into the BALB/c nude mice. This cell property switch further corroborates that TRPV2 may play an important role in the initiation and development of ESCC.

In organisms or the cells, thermal stress may exert effects on multiple signaling pathways [49–51], but we focused on the TRPV2-related pathways. We found that at least 3 pathways were activated during the overactivation of TRPV2, including HSPs (HSP70, HSP27), TNF α and PI3K pathways. Overactivation of TRPV2 could activate the signal of PI3K and its downstream signals ((PDK1, mTOR and Akt1), while its negative regulator (PTEN) was simultaneously inhibited; thus, the PI3K signals were amplified. The PI3K pathways have been found to be involved in the progression of numerous cancer forms [52–54]. Two small molecular compounds, VS5584 (a pan-PI3K/mTOR kinase inhibitor) and oroxin B (a PI3K/mTOR inhibitor and PTEN activator), were used in the cellular proliferation assay to further verify these findings. As expected, both compounds could abolish the cellular proliferation of ESCC cells following overactivation of TRPV2 in the cells, which suggests that TRPV2-PI3K/mTOR may be used as a novel target for the prevention and treatment of ESCC.

We also assessed more than 200 ESCC patient samples, including fresh samples and paraffin slides, and found that TRPV2 was upregulated among >87% of the fresh tumor samples and >84% of the tumor slides compared with the non-tumor control samples. Previously, Zhou *et al* reported that overexpression of TRPV2 is associated with poor prognosis in patients with ESCC [55] and Atsushi proposed that TRPV2 is involved in the maintenance of CSCs (cancer stem cells) of ESCC [56]. Recently, Michihiro *et al* described that overexpression of TRPV2 in two ESCC cell lines (TE15 and KYSE170) and TRPV2 strong expression is associated with a worse prognosis in ESCC patients [57]. These findings mutually confirmed with ours regarding the role of TRPV2 in driving the progression of ESCC. We further uncover a mechanism underlying the heat-challenging related pathogenesis of ESCC and provide new insight into the correlation of heat exposure on the esophageal mucosa with ESCC initiation and development.

Although great advances have been made in the detection and treatment of ESCC in the past decade, the outcomes of many patients still remain grim [58–60]; better preventive methods and therapeutic strategies are urgently needed for a better clinical prospect of ESCC patients. Our findings suggest that the temperature (54 °C) of thermal stimuli activating TRPV2 channel and driving the progress of ESCC is

much lower than the dietary temperatures among many populations, therefore, to advise the communities to stay away from high-temperature food could be an option.

Conclusions

To summarize, in this study, we found that the transient receptor potential vanilloid receptor 2 (TRPV2) was upregulated in ESCC cell lines and in ESCC tumor samples compared with non-tumor control subjects. Overactivation of TRPV2 promotes ESCC cancerous behaviors in vitro and enhances the tumorigenesis of ESCC in vivo. The protumorigenic role of TRPV2 was found to occur mainly via mediation of the PI3K/Akt/mTOR signaling pathway. Our current study, for the first time, reveals an important mechanism underlying the progression of ESCC upon thermal stress and uncovers the TRPV2-PI3K/Akt/mTOR pathway as a promising target for the prevention and treatment of ESCC. On the basis of our findings and the applicability of tranilast in clinic, a cooperative investigation has been initiated, aiming at translating this drug into clinical ESCC trials.

Abbreviations

TRPV2 (or VR2 or V2): transient receptor potential vanilloid receptor 2; ESCC:Esophageal squamous cell carcinoma; WT:wild-type; PBS:Phosphate Buffer Saline; HBSS:Hank's balanced salt solution; pDNA:plasmid DNA; CRISPR-Cas9:clustered regularly interspaced short palindromic repeats/CRISPR-associated nuclease 9; sgRNA:single-guide RNA; POT:point of off target; Eca-109-TRPV2^{-/-} (or VR2^{-/-} or V2^{-/-}):TRPV2 knocked-out Eca-109 cell line; DMSO:dimethyl sulfoxide; GFP:Green Fluorescent protein; gl:GFP- luciferase dually labeled; HUVECs:human umbilical vein endothelial cells; GIBH:Guangzhou Institutes of Biomedicine and Health; IF:Immunofluorescence; IHC:Immunohistochemistry; HE:hematoxylin-eosin; PI3K:phosphatidylinositol 3-kinase; AKT:V-Akt Murine Thymoma Viral Oncogene Homolog 1; mTORC1:mechanistic target of rapamycin complex 1; PTEN:Phosphatase and Tensin Homolog; HSP:heat shock protein; HIF1:hypoxia-inducible factor 1; PDK1:phosphoinositide-dependent protein kinase-1; MTT:3-(4,5-dimethylthiazol-2-yl)-2,5-diphenyltetrazolium bromide; CCK8:Cell counting kit-8; ns:Not significant

Declarations

Acknowledgements

We are grateful to Prof. GSW Tsao (Hong Kong University) for giving us the immortalized esophageal squamous cell line NE2 as a gift. We thank colleagues in GIBH, including Prof. Peng Li, Dr. Zhiwu Jiang for assistance in the establishment of GL-labeled cell lines, Dr. Kepin Wang, Dr. Jingke Xie for technical help with CRISPR-Cas9 editing and Prof. Huayu Qi for important comments on the manuscript.

Authors' contributions

Conception and design: Z.Y. Li, R.Q. Huang; Development of methodology: R.Q. Huang, S. Li, C. Tian, P. Zhou, H.F. Zhao, J. Xiao; Acquisition of data (provided animals, acquired and managed patients, provided facilities, etc.): Z.X. Lin, P. Zhou, W. Xie, J. Xiao, F. Tang; Analysis and interpretation of data (e.g., statistical analysis, biostatistics, computational analysis): R.Q. Huang, L. He, X.B. Han; Writing, review, and/or revision of the manuscript: R.Q. Huang, Z.Y. Li, Y.C. Yang;

Administrative, technical, or material support (i.e., reporting or organizing data, constructing databases): N. Cheng, H.L. Huang; Study supervision: Z.Y. Li; all authors reviewed and approved the final version of the manuscript.

Funding

This work was supported by Frontier Research Programs of Guangzhou Regenerative Medicine and Health Guangdong Laboratory (Grant No. 2018GZR110105020 and 2018GZR110105019), the National Natural Science Foundation of China (31671211), and the Science and Technology Planning Project of Guangdong Province, China (2017B030314056).

Availability of data and materials

All the data and materials supporting the conclusions were included in the main paper or as Supplemental Figures (1, 2, 3, 4, 5, 6 and 7), supplemental Tables (1 and 2) and associated figure legends are provided as supplemental material and are available online with the paper.

Ethics approval and consent to participate

All of the animal studies were conducted under protocols approved by the guidelines of the Ethics Committee of Animal Experiments at GIBH. For the use of clinical materials for this study, prior patient consent and approval from the Institutional Research Ethics Committee of the Cancer Hospital of Hunan Province and the Second Affiliated Hospital of Xiangya Medical School of Central South University were obtained.

Consent for publication

Written informed consent for publication was obtained from all authors.

Competing interests

The authors declare no conflict of interests.

References

1. Florea A, Sangaré L, Lowe K. A Multinational Assessment of Gastric, Esophageal, and Colorectal Cancer Burden: A Report of Disease Incidence, Prevalence, and Fatality. *J Gastrointest Cancer*. 2020;51(3):965–71.
2. Ferlay J, Shin HR, Bray F, Forman D, Mathers C, Parkin DM. Estimates of worldwide burden of cancer in 2008: GLOBOCAN 2008. *Int J Cancer*. 2010;127:2893–917.
3. Ma G, Zhang J, Jiang H, Zhang N, Zhu Y, Deng Y, et al. Microvessel density as a prognostic factor in esophageal squamous cell cancer patients: A meta-analysis. *Medicine (Baltimore)*. 2017; 96: e7600.
4. Domper Arnal MJ, Ferrández Arenas Á, Lanás Arbeloa Á. Esophageal cancer: risk factors, screening and endoscopic treatment in Western and Eastern countries. *World J Gastroenterol*. 2015;21:7933–43.
5. Xavier Castellsagué N, Munoz, Eduardo de Stefani. Influence of mate drinking, hot beverages and diet on esophageal cancer risk in south America. *Int. J. Cancer*. 2000; 88: 658–664.
6. Song Q, Jiang D, Wang H, Huang J, Liu Y, Xu C, et al. Chromosomal and genomic variations in esophageal squamous cell carcinoma: a review of technologies, applications, and prospections. *J. Cancer*. 2017; 8: 2492–2500.
7. McCormack VA, Menya D, Munishi MO, Dzamalala C, Gasmelseed N, Leon Roux M, et al. Informing etiologic research priorities for squamous cell esophageal cancer in Africa: A review of setting-specific exposures to known and putative risk factors. *Int. J. Cancer*. 2017; 140: 259–271.
8. Islami F, Boffetta P, Ren JS, Pedoeim L, Khatib D, Kamangar F. High-temperature beverages and foods and esophageal cancer risk-a systematic review. *Int. J. Cancer*. 2009; 125: 491–524.
9. Siegel R, Naishadham D, Jemal A. Cancer statistics. *CA Cancer J Clin*. 2012;62(1):10–29.
10. Enzinger PC, Mayer RJ. Esophageal cancer. *N Engl J Med*. 2003;349(23):2241–52.
11. Abnet CC, Arnold M, Wei WQ. Epidemiology of Esophageal Squamous Cell Carcinoma. *Gastroenterology*. 2018;154(2):360–73.
12. Lin S, Xu G, Chen Z, Liu X, Li J, Ma L, et al. Tea drinking and the risk of esophageal cancer: focus on tea type and drinking temperature. *Eur. J. Cancer Prev*. 2020; doi: 10.1097/CEJ.0000000000000568 (Epub ahead of print).
13. Gao Y, Hu N, Han XY, Ding T, Giffen C, Goldstein AM, et al. Risk factors for esophageal and gastric cancers in Shanxi Province, China: a case-control study. *Cancer Epidemiol*. 2011; 35(6): e91-99.
14. Tai WP, Nie GJ, Chen MJ, Yaz TY, Guli A, Wuxur A, et al. Hot food and beverage consumption and the risk of esophageal squamouscell carcinoma: A case-control study in a northwest area in China. *Med (Baltim)*. 2017;96(50):e9325.
15. Loomis D, Guyton KZ, Grosse Y, Lauby-Secretan B, El Ghissassi F, Bouvard V, et al. International Agency for Research on Cancer Monograph Working Group, Carcinogenicity of drinking coffee, mate, and very hot beverages. *Lancet Oncol*. 2016;17(7):877–8.
16. Okaru AO, Rullmann A, Farah A, Gonzalez de Mejia E, Stern MC, Lachenmeier DW. Comparative oesophageal cancer risk assessment of hot beverage consumption (coffee, mate and tea): the

- margin of exposure of PAH vs very hot temperatures. *BMC Cancer*. 2018; 18(1): 236–246.
17. Islami F, Pourshams A, Nasrollahzadeh D, et al. Tea drinking habits, oesophageal cancer in a high risk area in northern Iran: population based case–control study. *BMJ*. 2009;338:b929.
 18. Michael Oresto Munishi, Rachel Hanisch, Oscar Mapunda, Theonest Ndyetabura, Arnold Ndaro, Joachim Schuz, Gibson Kibiki, Valerie McCormack. Africa's oesophageal cancer corridor: Do hot beverages contribute? *Cancer Causes Control*. 2015; 26(10):1477–1486.
 19. Islami F, Boffetta P, Ren JianSong, Pedoeim L, Khatib D, Kamangar F. High-temperature beverages and Foods and Esophageal Cancer Risk – A Systematic Review. *Int J Cancer*. 2009;125(3):491–524.
 20. Huang R, Wang F, Yang Y, Ma W, Lin Z, Cheng N, et al. Recurrent activations of transient receptor potential vanilloid-1 and vanilloid-4 promote cellular proliferation and migration in esophageal squamous cell carcinoma cells. *FEBS Openbio*. 2019;9(2):206–25.
 21. Ma W, Li C, Yin S, Liu J, Gao C, Lin Z, et al. Novel role of TRPV2 in promoting the cytotoxicity of H₂O₂-mediated oxidative stress in Human hepatoma cells. *Free Radic BiolMed*. 2015;89:1003–13.
 22. Han W, Cao F, Ding W, Gao XJ, Chen F, Hu YW, et al. Prognostic value of SPARCL1 in patients with colorectal cancer. *Oncol Lett*. 2018;15(2):1429–34.
 23. Xie J, Ge W, Li N, Liu Q, Chen F, Yang X, et al. Efficient base editing for multiple genes and loci in pigs using base editors. *Nat Commun*. 2019;10(1):2852–65.
 24. Bae S, Park J, Kim JS. Cas-OFFinder: a fast and versatile algorithm that searches for potential off-target sites of Cas9 RNA-guided endonucleases. *Bioinformatics*. 2014;30(10):1473–5.
 25. Nilius B, Owsianik G, Voets T, Peters JA. Transient receptor potential cation channels in disease. *Physiol Rev*. 2007;87(1):165–217.
 26. West AV, Wullkopf L, Christensen A, Leijnse N, Tarp JM, Mathiesen J, et al. Dynamics of cancerous tissue correlates with invasiveness. *Sci Rep*. 2017;7:43800–13.
 27. Chiorazzi N, Ferrarini M. Cellular origin(s) of chronic lymphocytic leukemia: cautionary notes and additional considerations and possibilities. *Blood*. 2011;117(6):1781–91.
 28. Shin Y, Kim H, Han S, Won J, Jeong HE, Lee ES, et al. Hydrogels: Extracellular Matrix Heterogeneity Regulates Three-Dimensional Morphologies of Breast Adenocarcinoma Cell Invasion. *Advanced Healthcare Materials*. 2013;2(1):920–0.
 29. Huang YL, Segall JE, Wu M. Microfluidic modeling of the biophysical microenvironment in tumor cell invasion. *Lab Chip*. 2017;17(19):3221–33.
 30. Maciaczyk D, Picard D, Zhao L, Koch K, Herrera-Rios D, Li G, et al. CBF1 is clinically prognostic and serves as a target to block cellular invasion and chemoresistance of EMT-like glioblastoma cells. *Br J Cancer*. 2017;117(1):102–12.
 31. Caporali S, Amaro A, Levati L, Alvino E, Lacal PM, Mastroeni S, et al. miR-126-3p down regulation contributes to dabrafenib acquired resistance in melanoma by up-regulating ADAM9 and VEGF-A. *J. Exp. Clin. Cancer Res*. 2019; 38(1): 272–288.
 32. Hanahan D, Weinberg RA. Hallmarks of cancer: the next generation. *Cell*. 2011; 144(5): 646–74.

33. Brünnert D, Langer C, Zimmermann L, Bargou RC, Burchardt M, Chatterjee M, et al. The heat shock protein 70 inhibitor VER155008 suppresses the expression of HSP27, HOP and HSP90 β and the androgen receptor, induces apoptosis, and attenuates prostate cancer cell growth. *J. Cell Biochem.* 2020; 121(1): 407–417.
34. Jin HO, Hong SE, Kim JY, Kim MR, Chang YH, Hong YJ, et al. Induction of HSP27 and HSP70 by constitutive overexpression of Redd1 confers resistance of lung cancer cells to ionizing radiation. *Oncol Rep.* 2019;41(5):3119–26.
35. Söderström HK, Kauppi JT, Oksala N, Paavonen T, Krogerus L, Räsänen J, et al. Overexpression of HSP27 and HSP70 is associated with decreased survival among patients with esophageal adenocarcinoma. *World J Clin Cases.* 2019;7(3):260–9.
36. Shen J, Xiao Z, Zhao Q, Li M, Wu X, Zhang L, et al. Anti-cancer therapy with TNF α and IFN γ : A comprehensive review. *Cell Prolif.* 2018;51(4):12441.
37. Mickle AD, Shepherd AJ, Mohapatra DP. Sensory TRP channels: the key transducers of nociception and pain. *Prog Mol Biol Transl Sci.* 2015;131:73–118.
38. Benham CD, Gunthorpe MJ, Davis JB. TRPV channels as temperature sensors. *Cell Calcium.* 2003; 33(5–6): 479 – 87.
39. Dawood S, Austin L, Cristofanilli M. Cancer stem cells: implications for cancer therapy. *Oncology (Williston Park).* 2014;28(12):1101–7.
40. Toh TB, Lim JJ, Chow EK. Epigenetics in cancer stem cells. *Mol Cancer.* 2017;16(1):29.
41. Nassar D, Blanpain C. Cancer stem cells: basic concepts and therapeutic implications. *Annu Rev Pathol.* 2016;23(11):47–76.
42. Boussommier-Calleja A, Li R, Chen MB, Wong SC, Kamm RD. Microfluidics: A new tool for modeling cancer-immune interactions. *Trends Cancer.* 2016;2(1):6–19.
43. Chaicharoenaudomrung N, Kunhorm P, Noisa P. Three-dimensional cell culture systems as an *in vitro* platform for cancer and stem cell modeling. *World J Stem Cells.* 2019;11(12):1065–83.
44. Song HH, Park KM, Gerecht S. Hydrogels to model 3D *in vitro* microenvironment of tumor vascularization. *Adv Drug Deliv Rev.* 2014;79(80):19–29.
45. Levinger I, Ventura Y, Vago R. Life is three dimensional-as *in vitro* cancer cultures should be. *Adv Cancer Res.* 2014;121:383–414.
46. Shen CN, Goh KS, Huang CR, Chiang TC, Lee CY, Jeng YM, et al. Lymphatic vessel remodeling and invasion in pancreatic cancer progression. *EBioMedicine.* 2019;47:98–113.
47. Iwai S, Kishimoto S, Amano Y, Nishiguchi A, Matsusaki M, Takeshita A, et al. Three-dimensional cultured tissue constructs that imitate human living tissue organization for analysis of tumor cell invasion. *J Biomed Mater Res A.* 2019;107(2):292–300.
48. Harper SJ, Bates DO. VEGF-A splicing: the key to anti-angiogenic therapeutics. *Nat Rev Cancer.* 2008;8(11):880–7.

49. Abdelnour SA, Abd El-Hack ME, Khafaga AF, Arif M, Taha AE, Noreldin AE. Stress biomarkers and proteomics alteration to thermal stress in ruminants: a review. *J Therm Biol.* 2019;79:120–34.
50. Somero GN. The cellular stress response and temperature: Function, regulation, and evolution. *J Exp Zool A Ecol Integr Physiol.* 2020;333(6):379–97.
51. Burtscher M, Gatterer H, Burtscher J, Mairböurl H. Extreme Terrestrial Environments: Life in Thermal Stress and Hypoxia - A Narrative Review. *Front Physiol.* 2018;9:572.
52. Su T, Huang L, Zhang N, Peng S, Li X, Wei G, et al. FGF14 Functions as a Tumor Suppressor through Inhibiting PI3K/AKT/mTOR Pathway in Colorectal Cancer. *J Cancer.* 2020;11(4):819–25.
53. Wang JX, Jia XJ, Liu Y, Dong JH, Ren XM, Xu O, et al. Silencing of miR-17-5p suppresses cell proliferation and promotes cell apoptosis by directly targeting PIK3R1 in laryngeal squamous cell carcinoma. *Cancer Cell Int.* 2020;20:14.
54. Vasan N, Toska E, Scaltriti M. Overview of the relevance of PI3K pathway in HR-positive breast cancer. *Ann Oncol.* 2019;30:suppl 10: x3–11.
55. Zhou K, Zhang SS, Yan Y, Zhao S. Overexpression of transient receptor potential vanilloid 2 is associated with poor prognosis in patients with esophageal squamous cell carcinoma. *Med Oncol.* 2014;31(7):17.
56. Shiozaki A, Kudou M, Ichikawa D, Fujiwara H, Shimizu H, Ishimoto T, et al. Esophageal cancer stem cells are suppressed by tranilast, a TRPV2 channel inhibitor. *J Gastroenterol.* 2018;53(2):197–207.
57. Michihiro K, Atsushi S, Yuzo Y, Keita K, Toshiyuki K, Katsutoshi S, et al. The Expression and Role of TRPV2 in Esophageal Squamous Cell Carcinoma. *Sci Rep.* 2019;9(1):16055.
58. Lu YF, Yu JR, Yang Z, Zhu GX, Gao P, Wang H, et al. Promoter hypomethylation mediated upregulation of MicroRNA-10b-3p targets FOXO3 to promote the progression of esophageal squamous cell carcinoma (ESCC). *J Exp Clin Cancer Res.* 2018;37(1):301.
59. Hong Y, Ding ZY. PD-1 Inhibitors in the Advanced Esophageal Cancer. *Front Pharmacol.* 2019;10:1418.
60. Hirano H, Kato K. Systemic treatment of advanced esophageal squamous cell carcinoma: chemotherapy, molecular-targeting therapy and immunotherapy. *Jpn J Clin Oncol.* 2019;49(5):412–20.

Figures

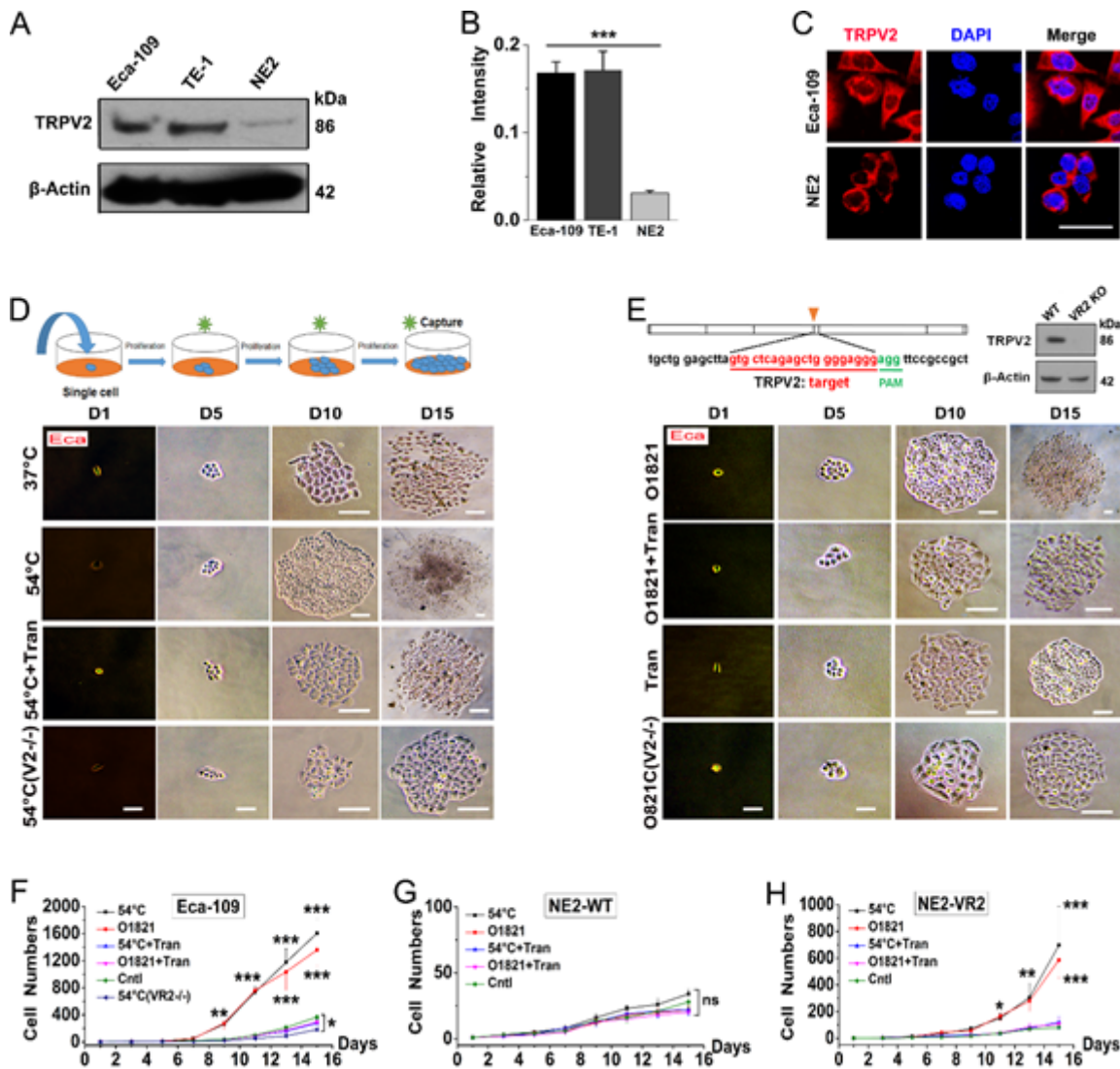


Figure 1

TRPV2 is upregulated in ESCC cells, and overactivation of TRPV2 promotes cellular proliferation. (a) Western blotting showing the expression pattern of TRPV2 (86 kDa) among ESCC cells (Eca-109 and TE-1) and non-tumor cells (NE2). β -Actin (42 kDa) was used as an internal control. (b) Densitometric quantification of TRPV2 protein among the three cell lines (n = 6). (c) ICF staining showing the expression of TRPV2 in Eca-109 and NE2 cells (TRPV2 in red) (n = 5). (d) Upper: outline of the single-cell culture assay for cellular proliferation. Lower: representative images of Eca-109 cells in the single-cell proliferation assay. Images were serially captured at 4-day intervals. (e) Upper: the targeted segment of the TRPV2 gene for CRISPR-Cas9 editing and western blotting showing that the knockout cells are devoid of TRPV2 protein. Lower: representative images of Eca-109 cells in the single-cell proliferation assay. (f) Eca-109 cell numbers were relative to the control cell numbers and plotted over a time course (n = 20 - 30). (g) Wild-type (WT) NE2 cell numbers were relative to the control cell numbers and plotted over a time course (n = 20 - 30). (h) Cell numbers of NE2 with ectopically expressed TRPV2 (VR2) were relative to the control cell numbers and plotted over a time course (n = 20 - 30). Eca: Eca-109; Cntl: control; Tran:

tranilast; Scale bar: 10 μ m. * $P < 0.05$, ** $P < 0.01$, *** $P < 0.001$ by student t tests for western blotting and two-way ANOVA tests for proliferation assay.

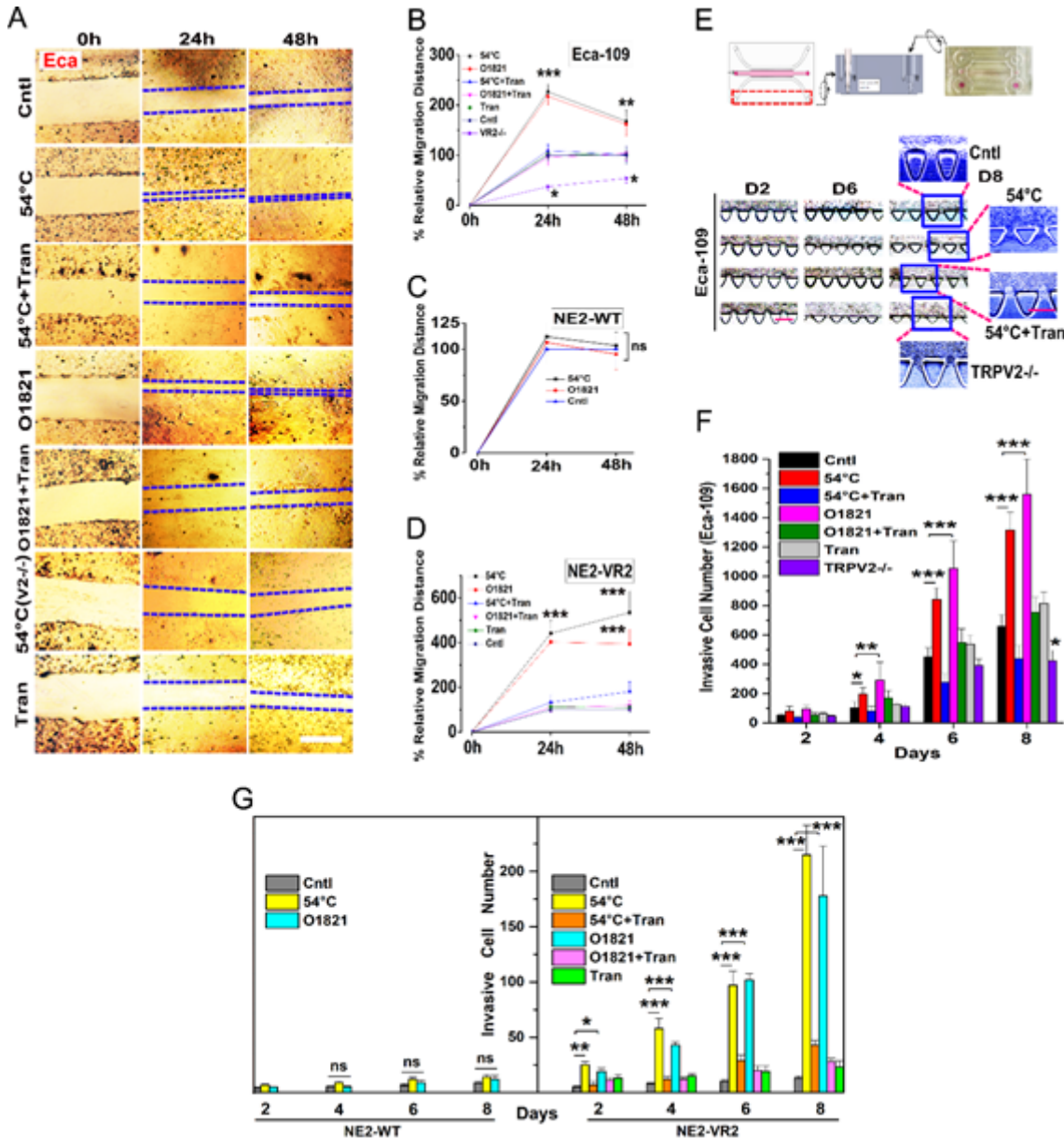


Figure 2

Overactivation of TRPV2 promotes the migration and invasion of ESCC and ectopically expressed TRPV2 NE2 cells. (a) Representative images of Eca-109 cell migration in the wound healing assay. (b) Cellular migration of Eca109 was promoted substantially by exposure to heat stimuli (54°C) or O1821 (20 μ M); these effects could be abrogated by tranilast (120 μ M) or by knockout of TRPV2 using CRISPR-Cas9 (n = 4). (c) Wild-type NE2 cell migration was affected neither by exposure to heat stimuli (54°C) nor by application of O1821 (20 μ M) (n = 3). (d) Migration of NE2 cells with ectopically expressed TRPV2 was enhanced markedly by exposure to heat stimuli (54°C) or O1821 (20 μ M), and these effects were abrogated by tranilast (120 μ M) (n = 3). (e) Upper: Schematic diagram of the 3-D culturing assay for cellular invasion. Lower: Sample images of Eca-109 cells invading the Matrigel in the 3D culture assay. (f) Invasive cells (Eca-109) were counted under a microscope, and the count were averaged, plotted against

a time course (n = 4). (g) Invasive cells of wild-type NE2 (WT) and NE2 with ectopically expressed TRPV2 (VR2) were counted under a microscope, and the count were averaged, plotted against a time course (n = 3). Eca: Eca-109; Cntl: control; Tran: tranilast; TRPV2^{-/-} (or V2^{-/-}): TRPV2 knocked-out Eca-109 cell line; Scale bar: 1.0 mm. *P < 0.05, **P < 0.01, ***P < 0.001 by two-way ANOVA tests.

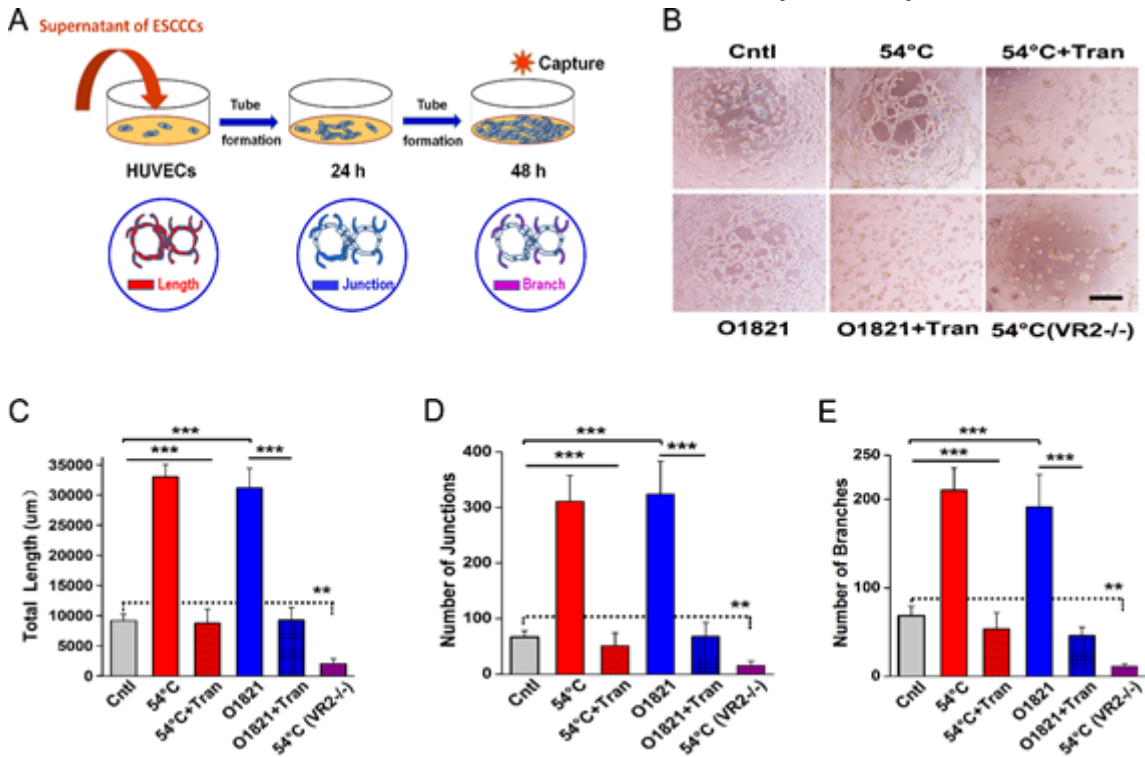


Figure 3

Overactivation of TRPV2 in ESCC cells promotes tumor-associated angiogenesis. (a) Schematic diagram of the tube formation assay. (b) Representative images of tube formation. (c) The effect of overactivation of TRPV2 on the total length of the newly formed microvessels (n = 3). (d) The impact of overactivation of TRPV2 on the junction numbers of the newly formed microvessels (n = 3). (e) The effect of overactivation of TRPV2 on the branch numbers of the newly formed microvessels (n = 3). HUVECs: human umbilical vein endothelial cells; Cntl: control; Tran: tranilast; VR2^{-/-}: TRPV2 knocked-out Eca-109 cell line; Scale bar: 20 µm. **P < 0.01, ***P < 0.001 by two-way ANOVA tests.

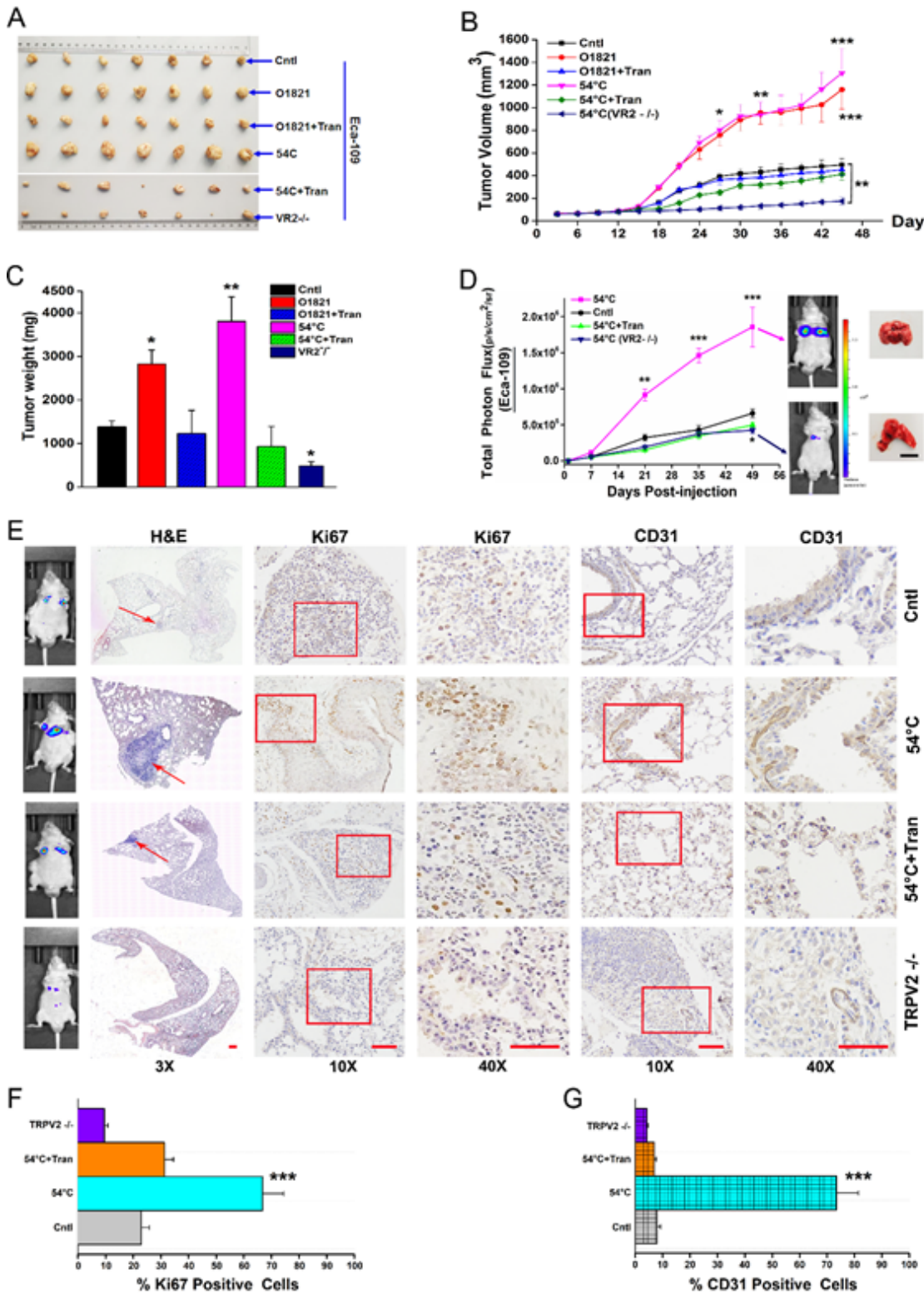


Figure 4

Overactivation of TRPV2 promotes ESCC formation and invasion in nude mice. (a) Representative images of the tumors formed in mice in each group. (b) Tumor volumes were measured on the indicated days and plotted over time ($n = 2$). (c) Mean tumor weights were compared between different groups ($n = 2$). (d) Photon flux was measured on the indicated days and plotted over time. Representative images of tumor-bearing mice and lungs from mice in the control group and the group followed heat (54°C) stimuli

in ESCC cells are shown on the right (n = 2). (e) H&E and IHC staining exhibited that overactivation of TRPV2 promoted the ESCC cells invasion into the lungs and promoted cellular proliferation and angiogenesis in the lungs, as indicated by percentages of Ki-67- f and CD31- g positive cells, respectively, whereas pharmaceutical inhibition or knockout of TRPV2 reduced all these indices (n = 5). Cntl: control; Tran: tranilast; TRPV2^{-/-} (or VR2^{-/-}): TRPV2 knocked-out Eca-109 cell line; Scale bar: 5 mm (in D); 500 μm (in E 3x and 10x); 250 μm (in E 40x). *P < 0.05, **P < 0.01, ***P < 0.001 by two-way ANOVA tests.

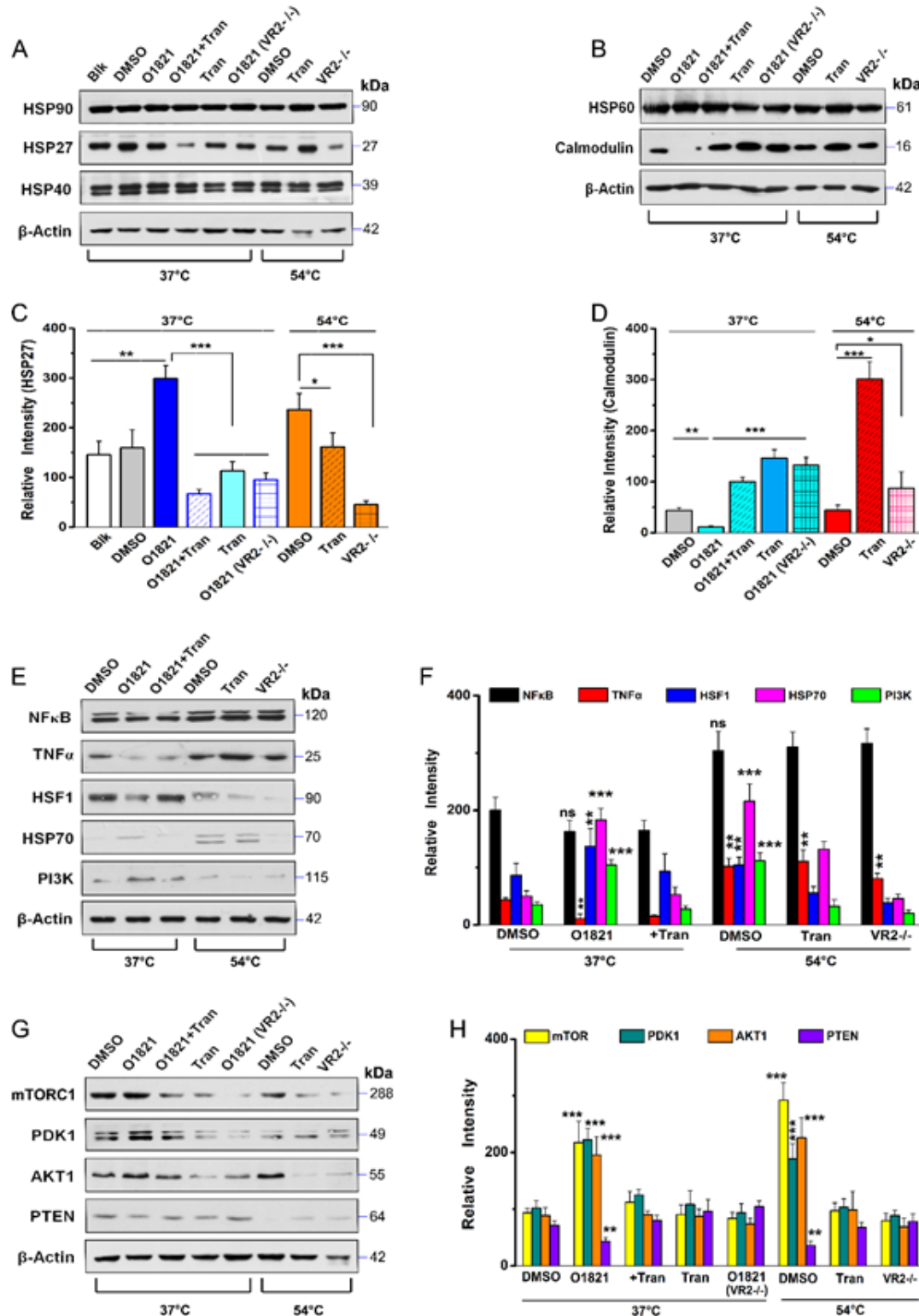


Figure 5

TRPV2 activation mediates HSP and PI3K signaling pathways. (a) Proteins levels of the HSP90, HSP40 and HSP27 were measured via western blotting. β -Actin was used as an internal control. (b) Protein levels of HSP60 and calmodulin were measured via western blotting. (c) Densitometric quantification of HSP27 protein, which was normalized relative to β -Actin and compared (n = 4). (d) Densitometric quantification of calmodulin protein, which was normalized relative to β -Actin and compared (n = 4). (e) Protein levels of HSF1, HSP70, NFKB, TNF α and PI3K were measured via western blotting. (f) Densitometric quantification of proteins in e, which were normalized relative to β -Actin and compared (n = 3 - 5). (g) PI3K signaling pathway related proteins were measured via western blotting. (h) Densitometric quantification of proteins in g, which were normalized relative to β -Actin and compared (n = 3 - 5). Blk: blank; DMSO: dimethyl sulfoxide; Tran: tranilast; VR2 $^{-/-}$: TRPV2 knocked-out Eca-109 cell line; *P < 0.05; **P < 0.01; ***P < 0.001, by two-way ANOVA tests.

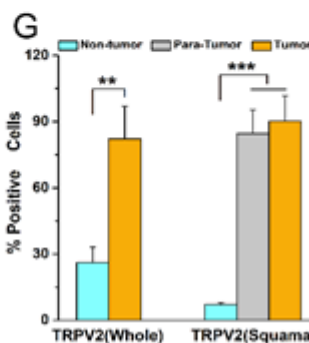
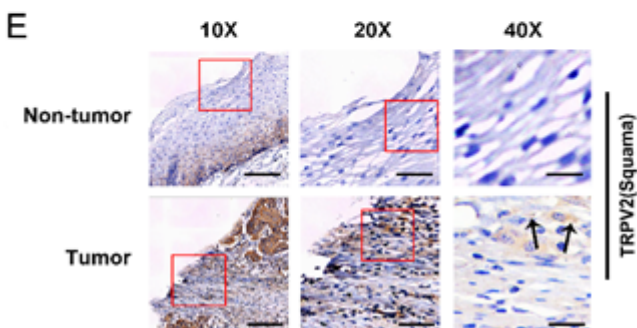
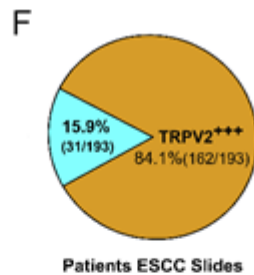
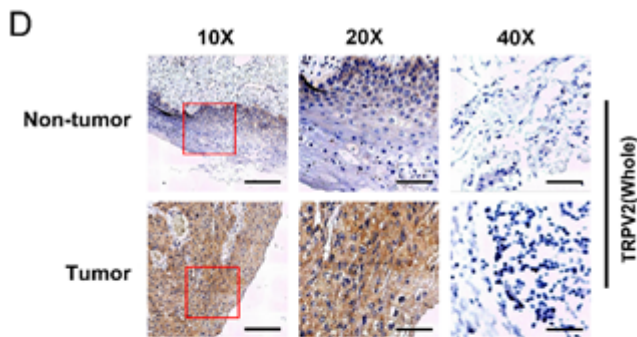
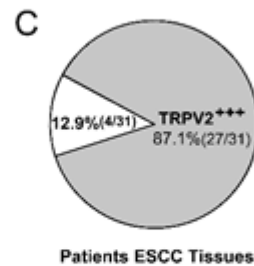
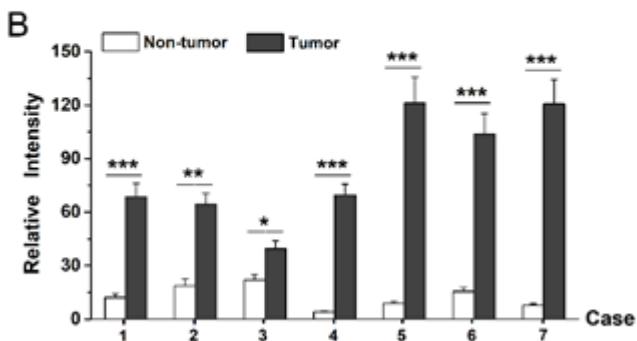
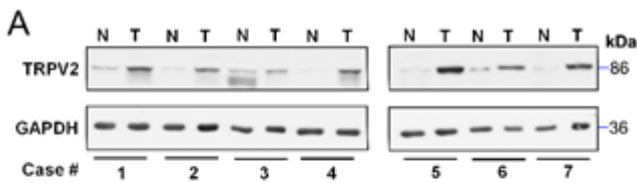


Figure 6

TRPV2 expression profile in ESCC patients. (a) Samples from ESCC and adjacent non-tumor tissues which were obtained during surgical procedures were subjected to western blotting to measure the expression of TRPV2. GAPDH was used as an internal control. Seven ESCC cases are shown here. (b) Densitometric quantification of TRPV2 protein among ESCC and adjacent non-tumor tissues (n = 3). (c) Percentage of TRPV2 upregulation (TRPV+++) among ESCC patients (fresh tumor samples) are shown. (d) Immunohistochemistry of slides of ESCC and adjacent non-tumor tissues from ESCC patients to detect the expression profile of TRPV2. Selected fields of the slides are magnified at 20x and shown. The rightmost microphotographs are derived from a negative control group (40x). (e) Immunohistochemistry of slides of ESCC and adjacent non-tumor tissues from ESCC patients to detect the expression profile of TRPV2. The fields of the squama in both para-tumor area of the ESCC slides and adjacent non-tumor slides were magnified at 20X and further at 40X and shown. (f) Percentage of TRPV2 upregulation (TRPV+++) among ESCC patients (paraffin tumor slides) are shown. (g) Summary of TRPV2-positive cells in d and e (n = 193). Scale bar: 50 μm at 10x, 25 μm at 20x and 12.5 μm at 40x. *P < 0.05; **P < 0.01; ***P < 0.001, by paired Student's t test or one-way ANOVA tests.